

Whistler turbulence in high beta plasma: Particle-In-Cell simulation

Shinji Saito¹, S. Peter Gary²

¹Solar-Terrestrial Environment Laboratory, Nagoya University, Furo-cho, Chikusa-ku, Nagoya 464-8601, Japan
saito@stelab.nagoya-u.ac.jp

²Los Alamos National Laboratory, Los Alamos, New Mexico 87545, USA
pgary@lanl.gov

Abstract

Solar wind observations show steeper magnetic spectra at electron scales than at proton scales. Earlier two-dimensional particle-in-cell (PIC) simulations of whistler turbulence in low beta plasmas demonstrated a cascade of magnetic fluctuation energy which is forward and anisotropic with preferential transfer of energy to wavevectors quasi-perpendicular to the background magnetic field. These simulations showed a magnetic wavenumber spectrum with a power-low index similar to that observed in the solar wind at electron scales. Here for the first time two-dimensional PIC simulation of whistler turbulence in high beta as observed in the solar wind at 1AU is carried out in a collisionless, homogeneous, magnetized plasma. Our simulation results show that the wavenumber anisotropy and the power-law index in high beta plasma are more isotropic and steeper than those in lower beta plasmas. Electron Landau and cyclotron damping become more effective at higher beta plasmas, so this simulation, that corresponds to solar wind conditions at 1 AU, suggests that electron kinetic effects are important in determining the properties of whistler turbulence in the high beta regime.

1. Introduction

Solar wind observations of plasma turbulence at 1 AU show magnetic power-law spectra with the Kolmogorov scaling $f^{5/3}$ in magnetohydrodynamic (MHD) regime where the observed frequency f is less than 0.2Hz [e.g. 1], which is called the “inertial range”. Around the observed frequency $\sim 0.2\text{Hz}$ where the MHD approximation is no longer valid, there is a spectral breakpoint. The magnetic spectra become steeper above this breakpoint [1-3], which is called the “dispersion/dissipation range”. Recent solar wind observations have shown that the spectral index in the range $0.5 < f < 20$ is between -2 and -3 [4-6]. Sahraoui *et al.* (2009) [4] found that there is a second spectral breakpoint with steeper magnetic spectra at $f > 20\text{Hz}$. The spectral breakpoint corresponds to electron scales $k\lambda_e \sim 1$ using the Taylor frozen-in-flow hypothesis in the solar wind at 1 AU, where λ_e is electron inertial length and k is wavenumber. Therefore above the second spectral breakpoint, electron kinetic effects would be important to understand fluctuation dissipation, electron heating, and short scale turbulence properties in the solar wind at 1 AU.

At electron scales, there are two competing fluctuations to describe short scale turbulence. One is kinetic Alfvén fluctuations which propagate in directions quasi-perpendicular to the background magnetic field with real frequencies $\omega_r < \Omega_p$, where Ω_p is the proton cyclotron frequency. Gyrokinetic simulations [7] show that the electric and magnetic wavenumber spectra of kinetic Alfvén turbulence have power-law indices of about -1/3 and -7/3 at proton scales (above the first spectral breakpoint) and leads to steeper wavenumber spectra at electron scales (above the second breakpoint). These electric and magnetic spectra are consistent with the recent solar wind observations at high frequencies [4], however other studies suggest that the kinetic Alfvén turbulence cannot completely represent the solar wind turbulence [8, 9]. A second type of fluctuations that can describe the short scale turbulence in the solar wind is whistler. Some aspects of whistler turbulence can be described by electron magnetohydrodynamics (EMHD) simulations which assume electrons to be a fluid and protons to be a stationary charge neutralizing background [10-13]. The EMHD simulations show a forward cascade of whistler fluctuations and magnetic wavenumber spectra that is proportional to $k^{-7/3}$ in both two- and three-dimensional simulations at scales $k\lambda_e < 1$. Anisotropic wavenumber spectra are also found, where the fluctuation energy is preferentially cascaded into fluctuations at quasi-perpendicular directions to the background magnetic field.

However, the solar wind observations at electron scales show steeper magnetic spectra than that predicted by the EMHD simulations if the Taylor frozen-in-flow hypothesis is valid. This suggests that whistler turbulence in the EMHD approximation cannot describe the short scale turbulence beyond the second breakpoint. The EMHD simulations do not represent the kinetic properties of the electrons, and therefore cannot correspond to the solar wind observations at 1 AU. In contrast, full particle-in-cell (PIC) simulations can demonstrate the kinetic properties of both electrons and protons.

Recent PIC simulations of decaying whistler turbulence show an anisotropic forward cascade of whistler turbulence [14-17]. These simulation results are qualitatively similar to the EMHD model. Previous PIC simulations use lower plasma beta than the solar wind plasma beta at 1 AU ($\beta \sim 1$), in order to understand essential properties of whistler turbulence, by keeping the electron Landau and cyclotron damping weak. To understand whistler turbulence in the solar wind at 1 AU, including relatively strong dissipation processes for whistlers at $k\lambda_e \sim 1$, the particle-in-cell simulations should be extended to $\beta=1$ regime. In this paper, we describe a two-dimensional particle-in-cell simulation including electron kinetic effects and show properties of decaying whistler turbulence at $\beta=1$.

2. Simulation model

The simulation code used here is the relativistic electromagnetic particle-in-cell code, which is modified from the TRISTAN code [18]. Our code calculates three-dimensional velocity space response of each proton and electron super-particles in two spatial dimensions. Hence, our simulation includes full kinetic properties of plasma, contrary to other fluid simulation models such as MHD and EMHD simulations. The simulation box size is $L_{\parallel} = L_{\perp} = 102.4\lambda_e$, where the electron inertial length contains 10 spatial grid points and subscript \parallel and \perp mean directions parallel and perpendicular to the background magnetic field (which are the horizontal and vertical directions in two dimensional system), respectively. The periodic boundary conditions for both directions are imposed on particles and electromagnetic fields. The total number of proton and electron super-particle pairs is about 6.7×10^7 . Other initial physical dimensionless parameters are mass ratio $m_p/m_e = 1836$, temperature ratio $T_p/T_e = 1$, plasma beta $\beta_p = \beta_e = 1$, and thermal speed $v_{e,th}/c = 0.1$ and $v_{p,th}/c = v_{e,th}(m_p/m_e)^{-1/2}$, where subscripts “ p ” and “ e ” mean proton and electron, respectively, and c is the light speed.

We impose 42 right-hand polarized whistler fluctuations at the initial time $t = 0$ in a homogeneous plasma. These wavenumbers are $k_{\parallel}\lambda_e = \pm 0.0613, \pm 0.1227$, and ± 0.184 , and $k_{\perp}\lambda_e = 0, \pm 0.0613, \pm 0.1227$, and ± 0.184 . Frequencies for the fluctuations are derived from the linear dispersion relation in a homogeneous collisionless plasma with physical parameters shown above. The magnetic fluctuations at $t=0$ satisfy

$$\delta\mathbf{B}(\mathbf{x}, t=0) = \sum_{n=1}^{42} \delta B_n \cos(\mathbf{k}_n \cdot \mathbf{x} + \phi_n) \quad (1)$$

where ϕ_n is generated by a random function between 0 and π , and n is a number of each mode. The electric field $\delta\mathbf{E}$ and electric current density $\delta\mathbf{J}$ of each mode satisfy Faraday's and Ampère's equations, where the electric current density is carried only by electrons ($\delta\mathbf{J} = -qn_e\delta\mathbf{v}_e$ assuming protons are at rest due to their large inertia in this relatively high frequency regime). At $t = 0$, each fluctuation has an equal fluctuating amplitude. The initial total magnetic fluctuation energy relative to the mean magnetic field energy $\sum_{n=1}^{42} (\delta B_n)^2 / B_0^2$ is equal to 0.1.

3. Simulation results

Figure 1 shows two-dimensional magnetic wavenumber spectra $|\delta\mathbf{B}(k_{\parallel}, k_{\perp})|^2 / B_0^2$ at $|\Omega_e|t = 0, \sim 212$, and ~ 424 . These panels clearly show a forward cascade that supplies fluctuation energy into larger wavenumbers. At $|\Omega_e|t \sim 212$, the forward cascade of the decaying whistlers shows an anisotropic wavenumber spectrum. The fluctuation energy is preferentially cascaded into quasi-perpendicular propagating whistlers. At a late time ($|\Omega_e|t \sim 424$), whistler fluctuations at relatively large wavenumbers are dissipated because of electron Landau and/or electron cyclotron resonances. The wavenumber spectrum becomes shrunken and looks more isotropic at the late time.

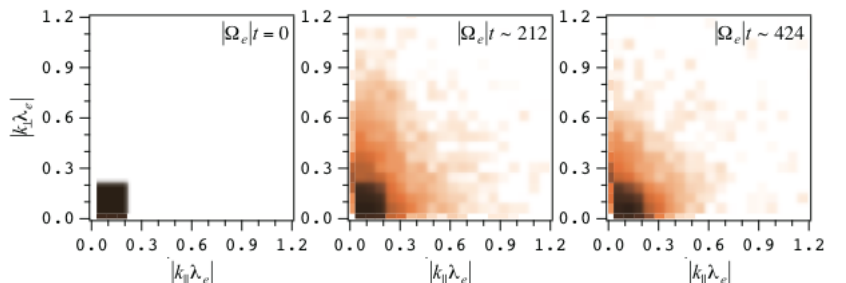


Figure 1: Magnetic wavenumber spectra $|\delta\mathbf{B}(k_{\parallel}, k_{\perp})|^2 / B_0^2$ at $|\Omega_e|t = 0, \sim 212$, and ~ 424 .

Figure 2 shows the time history of magnetic wavenumber anisotropy. The average wavevector anisotropy angle θ_B is defined as

$$\tan^2 \theta_B = \frac{k_y^2 |\delta\mathbf{B}(k_{||}, k_{\perp})|^2}{k_x^2 |\delta\mathbf{B}(k_{||}, k_{\perp})|^2} . \quad (2)$$

An isotropic spectrum corresponds to $\tan^2 \theta_B = 1$. We calculate $\tan^2 \theta_B$ over wavenumbers $0.3 \leq |k\lambda_e| \leq 3.0$ where $k = \sqrt{k_{||}^2 + k_{\perp}^2}$. The anisotropic forward cascade of magnetic fluctuations increases the anisotropy of developing whistler turbulence at earlier times ($|\Omega_e|t < 120$). The anisotropy has a maximum at $|\Omega_e|t \sim 120$, after which it gradually decreases. The maximum anisotropy in $\beta=1$ plasma seen in Figure 2 is clearly smaller than the anisotropy in $\beta=0.1$ as shown in Figure 2 of Saito *et al.* (2008) [15]. This suggests that whistler turbulence at high beta has more isotropic wavenumber spectrum than at low beta. As seen in Figure 1, the magnetic energy spectrum shrinks in the perpendicular wavenumber direction at later times, suggesting that the decrease of the isotropy is due to dissipation of whistler fluctuations propagating oblique directions. Linear theory suggests that electron Landau damping for obliquely propagating whistlers becomes stronger at higher beta, so the less anisotropic spectrum at $\beta=1$ could be explained by the electron Landau damping.

Figure 3 shows reduced wavenumber spectra as a function of the perpendicular wavenumber at $|\Omega_e|t \sim 212$ (red) and 424 (blue). The initially imposed fluctuations are at $|k_{\perp}\lambda_e| < 0.2$. The spectra show a power-law property with index of about -5.5, which is steeper than at low beta [15,17]. The spectral index is not strongly changed in time after whistler turbulence is well developed ($|\Omega_e|t > 100$). Even at $t \sim 120$ where the anisotropy has a maximum as seen in Figure 2, we confirmed that the spectral index is almost same. This indicates that the spectral index of the reduced wavenumber spectrum does not have a strong correlation with the wavenumber anisotropy.

4. Summary

We have done a two-dimensional particle-in-cell simulation to study whistler turbulence in $\beta=1$ condition that corresponds to the solar wind plasma beta at 1 AU. Our simulation results suggest that whistler turbulence has the steeper and more isotropic magnetic wavenumber spectrum in high beta plasma. Using a phenomenological turbulence expression that neglects dissipation effects, Saito *et al.* (2010) [17] predicted that the spectral index of whistler turbulence in the perpendicular wavenumber at electron scales is about -4. Our full kinetic simulation results show the steeper magnetic wavenumber spectrum than the theoretical one, suggesting that the electron kinetic effects including electron Landau and cyclotron damping lead to the steeper magnetic spectrum of whistler turbulence. Furthermore, energy dissipation in perpendicular wavenumbers leads to a less anisotropic wavenumber spectrum. This indicates that the electron kinetic processes are important in determining the properties of whistler turbulence in the solar wind at 1 AU.

5. References

1. C. W. Smith, B. J. Vasquez, and K. Hamilton, “Interplanetary magnetic fluctuation anisotropy in the inertial range”, *J. Geophys. Res.*, **111**, A09111, 2006.
2. R. J. Leamon, C. W. Smith, N. F. Ness, and W. H. Matthaeus, “Observational constraints on the dynamics of the interplanetary magnetic field dissipation range”, *J. Geophys. Res.*, **103**, 4775, 1998.

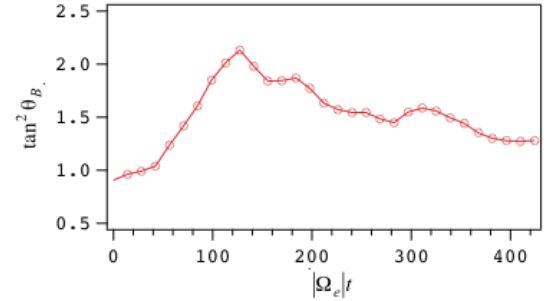


Figure 2: Time history of wavenumber anisotropy defined as Equation (1). The anisotropy is calculated in wavenumbers $0.3 \leq |k\lambda_e| \leq 3.0$.

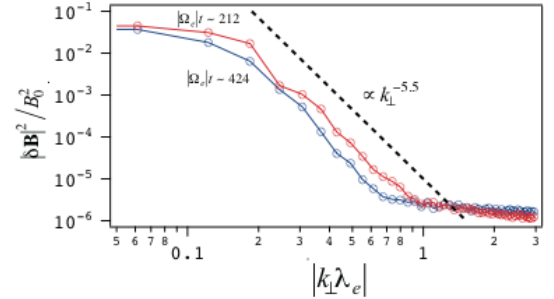


Figure 3: Reduced wavenumber spectra as a function of the perpendicular wavenumber at $|\Omega_e|t \sim 212$ (red) and 424 (blue). The dashed line is proportional to a power-law spectrum with the index -5.5.

3. O. Alexandrova, V. Carbone, P. Veltri, P. Veltri, and L. Sorriso-Valvo, “Small-scale energy cascade of the solar wind turbulence”, *Astrophys. J.*, **674**, 1153, 2008.
4. F. Sahraoui, M. L. Goldstein, P. Robert, and Y. V. Khotyaintsev, “Evidence of a cascade and dissipation of solar-wind turbulence at the electron gyroscale”, *Phys. Rev. Lett.*, **102**, 211102, 2009.
5. K. H. Kiyani, S. C. Chapman, Y. V. Khotyaintsev, M. W. Dunlop, and F. Sahraoui, “Global scale-invariant dissipation in collisionless plasma turbulence”, *Phys. Rev. Lett.*, **103**, 075006, 2009.
6. O. Alexandrova, J. Saur, C. Lacombe, A. Mangeney, J. Mitchell, S. J. Schwartz, and P. Robert, “Universality of solar-wind turbulent spectrum from mhd to electron scales”, *Phys. Rev. Lett.*, **103**, 165003, 2009.
7. G. G. Howes, W. Dorland, S. C. Cowley, G. W. Hammett, E. Quataert, A. A. Schekochihin, and T. Tatsuno, “Kinetic simulations of magnetized turbulence in astrophysical plasmas”, *Phys. Rev. Lett.*, **100**, 065004, 2008.
8. S. P. Gary and C. W. Smith, “Short-wavelength turbulence in the solar wind: Linear theory of whistler and kinetic Alfvén fluctuations”, *J. Geophys. Res.*, **114**, A12105, 2009.
9. J. J. Podesta, J. E. Borovsky, and S. P. Gary, “A kinetic Alfvén wave cascade subject to collisionless damping cannot reach electron scales in the solar wind at 1AU”, *Astrophys. J.*, **712**, 685, 2010.
10. D. Biskamp, E. Schwarz, and J. F. Drake, “Two-dimensional electron magnetohydrodynamic turbulence”, *Phys. Rev. Lett.*, **76**, 1264, 1996.
11. D. Biskamp, E. Schwarz, A. Zeiler, A. Celani, and J. F. Drake, “Electron magnetohydrodynamics turbulence”, *Phys. Plasmas*, **6**, 751, 1999.
12. S. Dastgeer, A. Das, P. Kaw, and P. H. Diamond, “Whistlerization and anisotropy in two-dimensional electron magnetohydrodynamic turbulence”, *Phys. Plasmas*, **7**, 571, 2000.
13. J. Cho and A. Lazarian, “The anisotropy of electron magnetohydrodynamic turbulence”, *Astrophys. J. Lett.*, **615**, L41, 2004.
14. S. P. Gary, S. Saito, and H. Li, “Cascade of whistler turbulence: Particle-in-cell simulations”, *Geophys. Res. Lett.*, **35**, L02104, 2008.
15. S. Saito, S. P. Gary, H. Li, and Y. Narita, “Whistler turbulence: Particle-in-cell simulations”, *Phys. Plasmas*, **15**, 102305, 2008.
16. S. P. Gary, S. Saito, and Y. Narita, “Whistler turbulence wavevector anisotropies: Particle-in-cell simulations”, *Astrophys. J.*, **716**, 1332, 2010.
17. S. Saito, S. P. Gary, and Y. Narita, “Wavenumber spectrum of whistler turbulence: Particle-in-cell simulation”, *Phys. Plasmas*, **17**, 122316, 2010.
18. O. Buneman. *Computer space plasma physics: Simulation techniques and software, chapter 3, page 67*, Terra Sci., 1993.